AIMS Environmental Science, 11(3): 360–379
DOI: 10.3934/environsci.2024017
Received: 25 February 2024
Revised: 10 April 2024
Accepted: 16 April 2024
Published: 29 May 2024

http://www.aimspress.com/journal/environmental

Research article

Fluoride removal from water using $Al(OH)_3$-surface modified diatomite mixed with brick: optimization, isotherm and kinetic studies

Isaiah Kiprono Mutai[1,2], Henry Kirimi Kiriamiti[1], Milton M M'Arimi[1] and Robert Kimutai Tewo[2,*]

[1] Department of Chemical and Process Engineering, Moi University, P.O. Box 3900-30100, Eldoret, Kenya

[2] Department of Chemical Engineering, Dedan Kimathi University of Technology, Private Bag–10143, Dedan Kimathi, Nyeri, Kenya

* **Correspondence:** Email: robert.tewo@dkut.ac.ke; Tel: +254723484716

Abstract: Excess fluoride in drinking water causes both dental and skeletal fluorosis among other problems. As such there is need to develop affordable and easily accessible techniques for fluoride removal from drinking water. This work assessed surface modified diatomite mixed with brick for fluoride removal. Diatomite samples were modified using aluminium hydroxide and the mixture was optimized for fluoride removal through response surface methodology (RSM) using the Box-Wilson central composite design. Batch experiments showed that, individually, a 28 g/L dose of the surface modified diatomite sufficiently removed fluoride to the acceptable level of 1.5 mg/L from an initial concentration of 10 mg/L fluoride while a 300 g/L dose of brick powder was required to remove an equal amount of fluoride in the same water samples. RSM optimization showed that a mixture of surface modified diatomite and brick in the mass ratio 1.8:17.8 grams per milligram of fluoride in water can be used to remove fluoride in water to an acceptable level. Adsorption of fluoride by surface modified diatomite fit better into the Freundlich adsorption isotherm (R^2=0.9753) compared to the Langmuir (R^2=0.8954), while adsorption by brick better fit the Langmuir adsorption mechanism (R^2=0.9804) in comparison to the Freundlich adsorption (R^2 =0.9372). Kinetic studies revealed that chemisorption was the main mechanism for both surface modified diatomite and brick adsorbents. Conclusively, an optimal mixture of surface modified diatomite and brick can be successfully used for fluoride removal in areas for which water has high fluoride contamination.

Keywords: fluoride; water; fluorosis; adsorption; optimization; isotherms; kinetics

1. Introduction

The presence of fluorides in drinking water is a subject that continues to attract attention globally. It is considered a double-edged sword in drinking water due to its positive and negative effects depending on its levels [1]. It is considered a safe and simple means of preventing dental caries in children when the levels are within the set standard, but detrimental to health, possibly resulting in dental fluorosis when the levels are above the recommended limits [2]. Several countries have set standards for fluoride in water in efforts to fight the devastating effects of low or excess fluoride in water. South Africa for example has a fluoride upper limit of 0.75 mg/L [3], while Malawi uses a previous WHO standard value of 6 mg/L [4]. The regional prevailing temperatures are among the key factors that determines the appropriate limits that various countries have set for fluoride in drinking water [5].

The current World Health Organization (WHO) acceptable limit of fluoride is 1.5 mg/L [6, 7]. It is noted that high levels of fluoride above this value have risks of dental and skeletal fluorosis [8]. Several countries have adopted this WHO standard as the guideline of fluoride in water, and Kenya is among them [9]. Despite legislation that regulates the fluoride levels in drinking water, cases of fluorosis are still reported in countries affected by fluoride contamination in water. In Kenya for example, cases of crippling fluorosis have been reported for more than a decade in some areas, such as those around Lake Baringo [10, 11]. The water from Lake Baringo has been reported to have fluoride levels as high as 5.2 mg/L [12], while other parts of the country, such as Nakuru, have reported levels of up to 7.6 mg/L in piped water [13]. Therefore, more effort on fluoride removal in water is of great significance.

Currently, there are several techniques for removal of fluoride from contaminated water [14]. These methods include adsorptive and additive techniques, membrane filtration, electrodialysis, and advanced oxidation processes, among others, which fall into adsorption, ion-exchange, coagulation-precipitation, membrane processes, and biological methods [15]. Several works have been dedicated to the review of these methods, including the findings, merits, and demerits of each technique [16–18]. Among these methods, adsorption is considered a primary technique for water defluoridation [19]. This is due to its simplicity in design, ease of operating,and reusability of the adsorbent [15]. However, the cost of the adsorbents used in defluoridation is one of the challenges that derail the efforts of removal of excess fluoride in water.

Surface modification of commonly available adsorbents is promising in improving the adsorbents' ability to remove the contaminants in water. There are several surface modification techniques for the adsorbents, including protonation, metal and metal oxide impregnation, amine group grafting, use of organic compounds, and heat treatment, which are broadly grouped into chemical and physical techniques [20]. Several studies have been carried out on the modification of diatomite for its improvement as an adsorbent. Methods including thermal, hydrothermal, alkaline, and acid modification, among others, have been used, although the focus has been on the use for removal of dyes and metal ions in water [21]. Akafu et al. [22] applied surface modified diatomite for fluoride removal in water; however, there is still limited information on the use of surface modified diatomite for fluoride removal.

The goal of this work was to test the viability of a mixture of surface modified diatomite and bricks as cheap adsorbent for removal of fluoride from contaminated water. Diatomite is an abundantly available adsorbent in many locations. It is 500 times cheaper than activated carbon, yet as equally effective as activated carbon in filtration [22]. It is noted to have high voidage of 80-90% [23], with pore

size distribution of 10-200μm [22]. Diatomite fluoride removal capacity is low, but can be improved through surface modification. On the other hand, bricks have been found to remove fluoride in water due to the presence of oxides of elements including iron and aluminium [24, 25].

In this work, diatomite samples were modified using aluminium hydroxide and then tested for fluoride removal. Similarly, brick powder was studied for its fluoride removal. The mixture of both surface modified diatomite and brick were optimized for fluoride removal by response surface methodology (RSM) using central composite design (CCD).

2. Materials and methods

2.1. Surface modification of diatomite

The diatomite samples were collected from African Diatomite Industries Limited (ADIL) company in Gilgil, Nakuru county in Kenya. The samples were subjected to surface modification based on the procedure employed by Akafu and co-workers with some minor modifications introduced [22]. A mass of 100 grams of the raw diatomite sample was weighed and washed with distilled water to remove dirt. The washed samples were then transferred to 1 litre glass beakers and 400 ml of 1M aluminium chloride solution was added. An equal volume of 3M sodium hydroxide solution was immediately added to the mixture. The mixture was then stirred at 200 rpm for 4 hours using a magnetic stirrer. After 4 hours, the mixture was acidified to a pH of 2 using 0.1M hydrochloric acid, and then stirred for another 30 minutes. The solid obtained was then washed with distilled water with the aid of a vacuum filter until the pH of the supernatant was 6. The solid was then dried in an oven at 80°C for 12 hours. After the drying process, the dried solid was removed, covered with aluminium foil, and left to cool to room temperature. It was then crushed and sieved through a 280 μm sieve to obtain fine powder. The powder was then corked in a plastic container and kept ready for use.

2.2. Preparation of brick

Burnt clay red bricks were obtained from the brick making site in Kesses, near Moi University in Eldoret, Kenya. The collected bricks were crushed to reduce the particle sizes. The crushed particles of bricks were then passed through a 280 μm sieve to obtain a fine powder. The fine powder was kept in sealed polythene bag ready for use.

2.3. Adsorbent characterization

Samples of raw diatomite, modified diatomite, used diatomite, and brick were characterized for their surface morphology and elemental composition. Scanning electron microscopes (SEM) with energy dispersive x-ray (EDX) capability (CamScan 24 and CamScan 44) were used. About 1 cm^2 of the sample was mounted on flat aluminium stubs using a two-sided adhesive film to adhere the sample to the stub. The samples were then sputtered with a thin coating of gold layer using the Pirani 10 sputter coater (Edwards Sputter Coater S150B). The SEM was equipped with secondary electrons (SE) and backscattered electrons (BE) detectors, which enabled the microscopic observation. The microanalyses provided detailed information on the morphological characteristics and the elemental composition of the samples.

2.4. Preparation of fluoride solutions

A 1000 mg/L fluoride stock solution was prepared by dissolving 1.01 g of sodium fluoride (99% NaF, Loba Chemie Pvt. Ltd, India) in distilled water in a 1L volumetric flask, then diluting to the mark. Solutions containing 10 mg/L fluoride were then obtained through dilution of the stock solution using distilled water.

2.5. Determination surface modified diatomite and brick doses for fluoride removal

The amount of surface modified diatomite required to remove fluoride to a residual level of 1.5 mg/L from 10 mg/L was determined by dosing varied masses of the surface modified diatomite to 250 ml of 10 mg/L fluoride solution. Stirring was carried out for 1 hour in a batch process using a magnetic stirrer, at which point the residual fluoride in the water was measured using the Palintest method, a technique which is based on the zirconyl chloride and Eriochrome cyanine R method [26]. The ELE International Paqualab^{TM} Photometer (England) was used alongside the Palintest reagents (Fluoride AP179). This process was repeated for brick dosage to determine the mass of brick required to reduce the fluoride content to the WHO standard of 1.5 mg/L fluoride concentration.

2.6. Adsorbent mixture optimization

The mass ratio of the surface modified diatomite and brick was optimized through experimental design. The design of the experiment was done using Box-Wilson central composite design (CCD) of the response surface methodology (RSM). Design expert software version 13.0 was used. Central composite design was chosen due to its ability to predict optimized conditions accurately with a minimum number of runs [27]. In the design, five levels and two factors were used, which yielded a total of 13 experiments with 5 replications at the center points. Table 1 shows the independent variables and their levels for the experiment.

Table 1. Independent variables and their levels in CCD design. Codes: X_1-mass of modified diatomite (g), X_2-mass of brick (g)

	Variable Levels				
Variable	-α:-1.414	-1	0	1	α:1.414
X_1	0.237	5	16.5	28	32.864
X_2	10.294	60	180	300	349.706

The limits for the variables X_1 and X_2 were set as the masses of the adsorbents determined through the procedure in section 2.5 (28g and 300g, respectively). The value of α is as per the formula $\alpha = (2^k)^{0.25}$, where k is the number of factors [28].

2.7. Isotherm studies

2.7.1. Surface modified diatomite

The studies on isotherms were carried out for the surface modified diatomite by dosing 2g of the surface modified diatomite to 125 ml samples of water with varied concentrations of fluoride ions. The fluoride ion concentrations ranged from 100 mg/L to 5 mg/L. The mixtures were stirred for a

constant time of 30 minutes at a rate of 200 rpm, after which the equilibrium concentration of the F^- ions was measured using the photometer and recorded for each sample. All studies were carried out at room temperature (20°C) and a pH of 6. The results were analyzed and fitted to both Langmuir and Freundlich isotherms.

2.7.2. Brick

The studies on isotherms were carried out for brick by dosing 20 g of powdered brick to 125 ml samples of water with varied concentrations of fluoride ions. The fluoride concentration was 100 mg/L to 10 mg/L. The mixtures were stirred for a constant time of 30 minutes at a rate of 200 rpm. The equilibrium concentration of the F^- ions was then measured using the photometer and recorded for each sample. The experiments were conducted at room temperature (20°C) and a pH of 6. The results were analyzed and fitted to both Langmuir and Freundlich adsorption isotherms.

2.8. Kinetic studies

2.8.1. Surface modified diatomite

The kinetic studies for surface modified diatomite were carried out with the optimum mass of the surface modified diatomite. Mass of the adsorbent (3.5 g) was dosed in 125 ml of water samples containing 10 mg/L of F^- ions. Each water sample was stirred at a rate of 200 rpm for varied periods of time of 0 to 150 minutes. Residual fluoride concentration was determined after every set of time and recorded. The experiments were conducted at room temperature (20°C) and a pH of 6. The data collected was analyzed and fitted to both pseudo first-order and pseudo second-order kinetic models.

2.8.2. Brick

The kinetic studies for brick were carried out with the optimum mass of powdered brick. Mass of the brick (37.5 g) was dosed in 125 ml of water samples containing 10 mg/L of F^- ions. Each water sample was stirred at a rate of 200 rpm for varied periods of time of 0 to 135 minutes. Residual fluoride concentration was determined after every set of time and recorded. The experiments were conducted at room temperature (20°C) and a pH of 6. The data collected was analyzed and fitted to both pseudo first-order and pseudo second-order kinetic models.

3. Results and discussion

3.1. Diatomite morphology and EDX microanalysis

The microstructural features of diatomite in its raw, modified, and used forms were obtained by SEM imaging. The SEM micrographs of the raw diatomite samples are shown in Figure 1. The micrographs showed that the diatomite was mainly composed of centric diatom particles, but with presence of pinnate structures as well (Figure 1a). Figure 1a also shows high void volume in the structure. A close view of the particles (Figure 1b) shows high porosity in the diatomite particles. This agreed with the work done by Hong et al. who researched diatomite samples obtained from China. The authors found that diatomite was mainly composed of centric diatom particles with two discs attached to each other by circular girdle. In addition, they observed numerous skeletal pores and interparticle

pores between the diatom particles, which is akin to the high porosity of diatomite [29]. Similarly, Izuagie et al. found pinnate structures on the diatomite sourced from the Kariandusi mine in Kenya, with high porosity too [30].

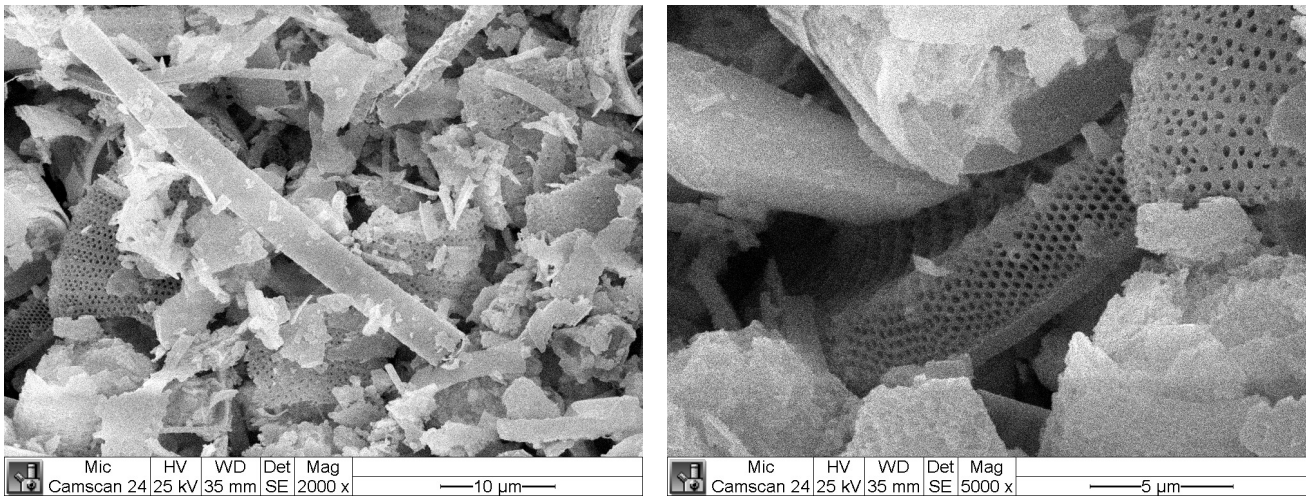

(a) **(b)**

Figure 1. SEM Images of the raw diatomite. (a) The images show a diverse structures in the material (b) The material depicts high porosity

Figure 2 shows the diatomite after modification of the surface with $Al(OH)_3$ (Figure 2a) and after use in the defluoridation process (Figures 2b and 2c). Figure 2a shows that a new layer has been attached to the surface of diatomite and the pore sizes were reduced after modification. This is an indication of successful surface modification. On the other hand, the clear features of diatomite emerge again on the used diatomite, which is an indicator that the layer formed during the surface modification was used up in the defluoridation process (Figure 2b). In addition, regular shaped deposits are observable on the surface of the used diatomite as seen in Figure 2c. This could be attributed to the deposits of aluminium fluoride (AlF_3) in some metastable phase. Metastable phases of AlF_3, such as γ, t, and ϵ, exist and may be indicative of the impure form or mixtures of beta phases [31].

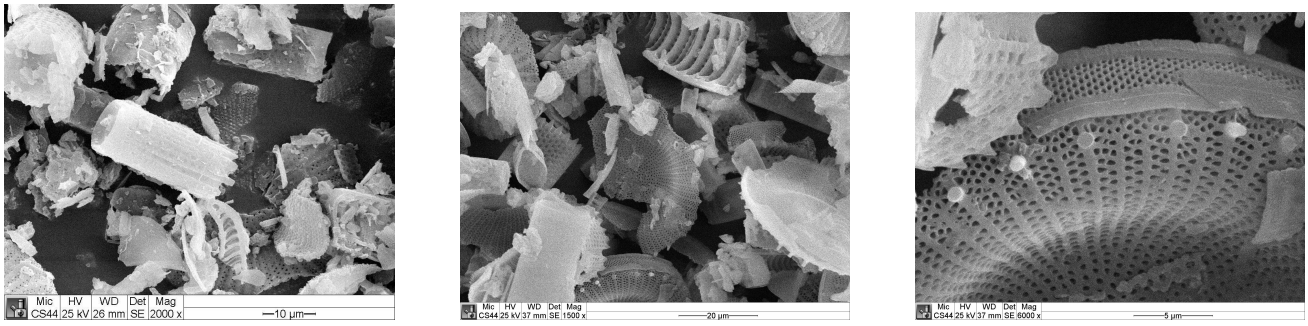

(a) **(b)** **(c)**

Figure 2. Surface morphology of the modified and the used diatomite. (a) Surface modified diatomite; a new layer has been attached to the surface and the pore sizes were reduced after modification (b) Used diatomite (c) New features identifiable on the used diatomite

Figure 3 shows the results of EDX analysis on the diatomite samples before and after modification. From Figure 3, raw diatomite was shown to have silicon (Si), aluminium (Al), potassium (K), calcium (Ca), iron (Fe), and oxygen (O). Silicon had the highest peaks in all the samples, which means its composition was highest. This is because diatomite is mainly composed of silica ($SiO_{2.n}$ H_2O) in its structure. Modification of the diatomite by $Al(OH)_3$ resulted in an increased composition of oxygen and aluminium, reduction in silicon composition, and introduction of chlorine (Cl) in the sample. On the other hand, the other elements, including K, Ca, and Fe, were not detected after modification of the diatomite sample. Similarly, the oxygen count in the sample further increased after the defluoridation process. However, the Al count after the defluoridation process decreased. The decrease in the Al count can be attributed to some of the ions being used in the defluoridation process. The increase in the oxygen count after modification and after the defluoridation process could be attributed to the oxygen coming from the water molecules retained in the silica or the alumina matrix of the diatomite, during diatomite modification as well as during the defluoridation process [32]. The absence of K, Ca and Fe after modification can be attributed to the ions of these elements replacing the aluminium in the aluminium chloride to form soluble chloride washed off in the solution at the time of diatomite modification. Chlorine in the modified diatomite is from the aluminium chloride and hydrochloric acid used in the modification process. Similarly, the reduction in the Si count after diatomite modification can be due to the removal of silicon ions by aluminium hydroxide and sodium hydroxide during the process of modification [33].

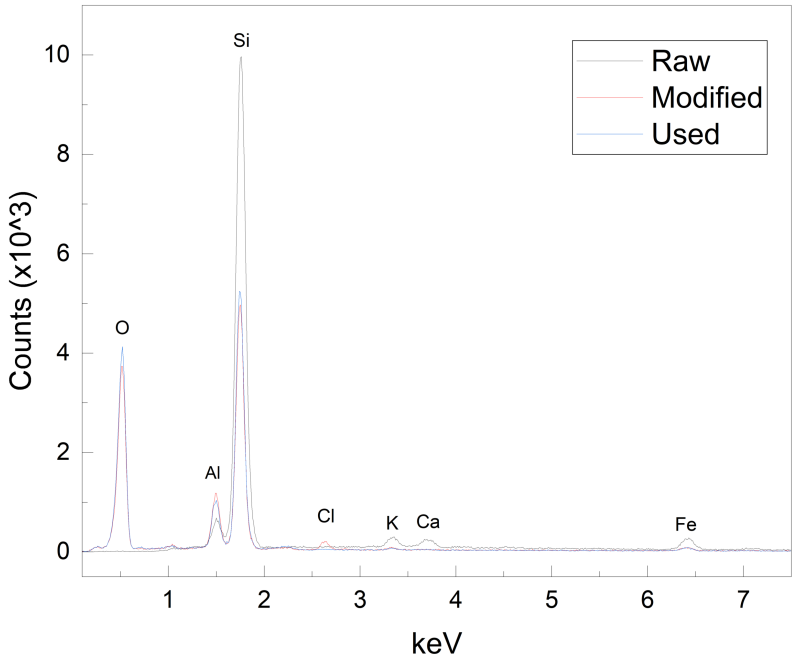

Figure 3. Diatomite EDX analyses for raw, modified, and used diatomite samples. The microanalyses shows a difference in elemental composition for the three samples.

3.2. Brick Morphology and EDX Microanalysis

Surface morphology of brick was studied using a scanning electron microscope to determine any unique features in its structure. The findings showed the presence of particulate matter distributed in its structure (Figure 4a). The presence of the space in between the particles is evidence of good porosity in the bricks. In addition to this, further focus on the structure of the particles in the brick revealed a structure similar to that of quartz (Figure 4b). This agreed with the findings of Ouyang et al. [34]. The study by Ouyang and coauthors compared the morphological structure of clay brick powder to commercial quartz and found that there was little difference in terms of morphological features between clay brick powder and quartz [34].

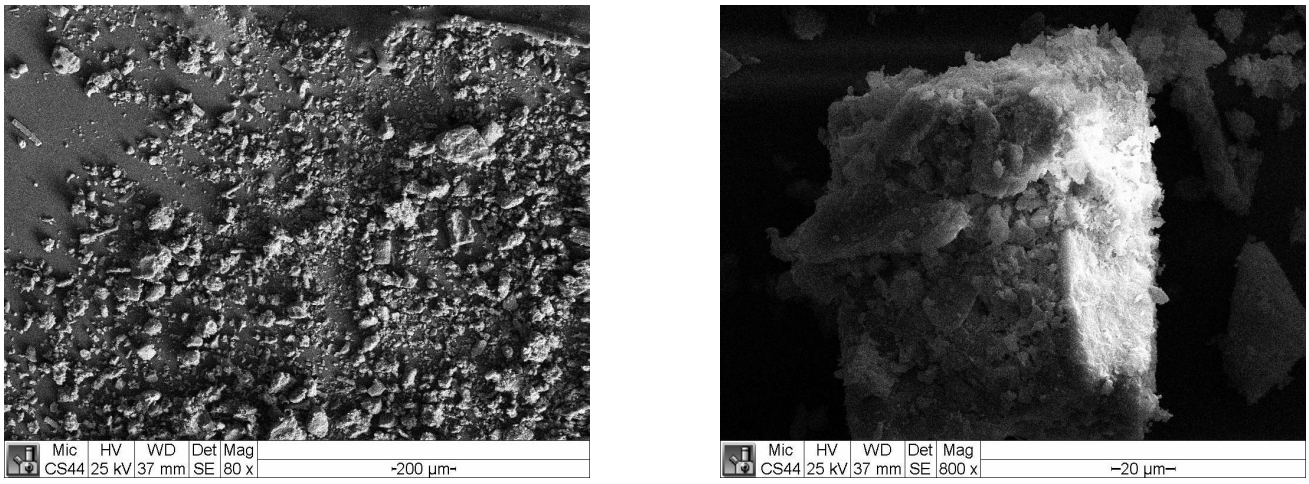

(a) **(b)**

Figure 4. Morphology and elemental analyses of brick. (a) Morphological analysis of brick through a scanning electron microscope. (b) A close view of brick particle structure.

The EDX analysis in the present study agreed with these findings by Ouyang et al. It is noted that a typical brick powder is a mixture of oxides of silicon, aluminium, iron, calcium, and magnesium [35]. On the other hand, quartz is composed of 98.8% silicon dioxide [34]. Figure 5 shows the EDX analysis of the brick sample. The presence of highest counts of silicon and oxygen respectively in Figure 5 confirms the composition of brick to be mainly quartz. It is however evident from Figure 5 that bricks have many other elements present including aluminium, titanium, selenium, potassium, and hafnium. Ouyang et al. found traces of calcium, magnesium, and sodium metals in addition to silicon dioxide in their clay brick powder [34]. The difference in the elemental composition of brick as revealed by the microanalyses of brick in different studies can be attributed to the difference in the soil compositions of the areas from which the bricks were sourced. The defluoridation capacity of brick is aided by this presence of the metal oxides in the brick, which interacts with the fluoride in water [35].

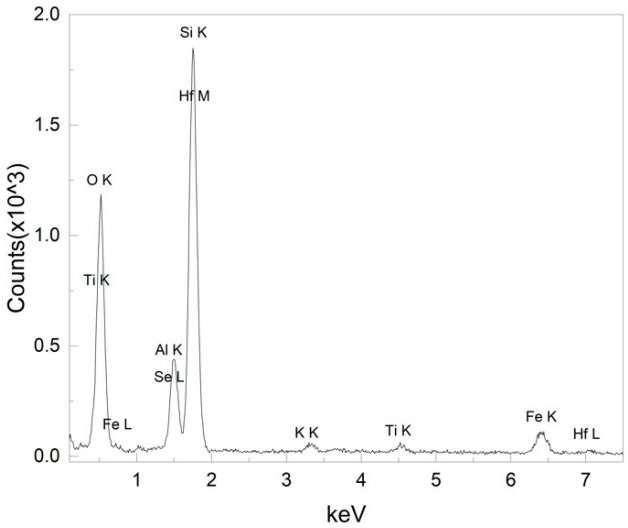

Figure 5. Energy dispersive x-ray chromatogram showing elemental analysis of brick.

3.3. Fluoride removal by diatomite and brick

The removal of fluoride in water by diatomite and brick was studied to determine the required doses of the individual adsorbents that can remove the fluoride to the WHO standard of 1.5 mg/L. In addition, the raw and modified diatomite samples were compared to determine the impact of surface modification of diatomite on fluoride removal. Figure 6 shows the fluoride removal by both diatomite and brick. From Figure 6a, the fluoride removal by raw diatomite is low. For a litre of water containing fluoride, at an initial concentration of 10 mg/L fluoride, 28 g of raw diatomite removes fluoride to a residual value of 9.5 mg/L. On the other hand, the surface modified diatomite is very effective. A similar dose of the modified diatomite under the same conditions removes fluoride effectively to 1.5 mg/L. This was the optimum dose for the modified diatomite for removal of fluoride in water. With similar initial concentration of fluoride of 10 mg/L, Akafu and coauthors found the optimum dosage of $Al(OH)_3$-surface modified diatomite to be 25 g/L [22]. The difference between the optimum values obtained by Akafu et al. and the present study could be due to the slight difference in diatomite modification procedures used. Figure 6b, indicated low fluoride removal in water by the use of brick as an adsorbent. To achieve a residual fluoride content of 1.5 mg/L, a total of 300 g/L dosage of the brick powder is required. Despite this low capacity, the low cost of brick and its ease of accessibility makes it of interest in defluoridation [35].

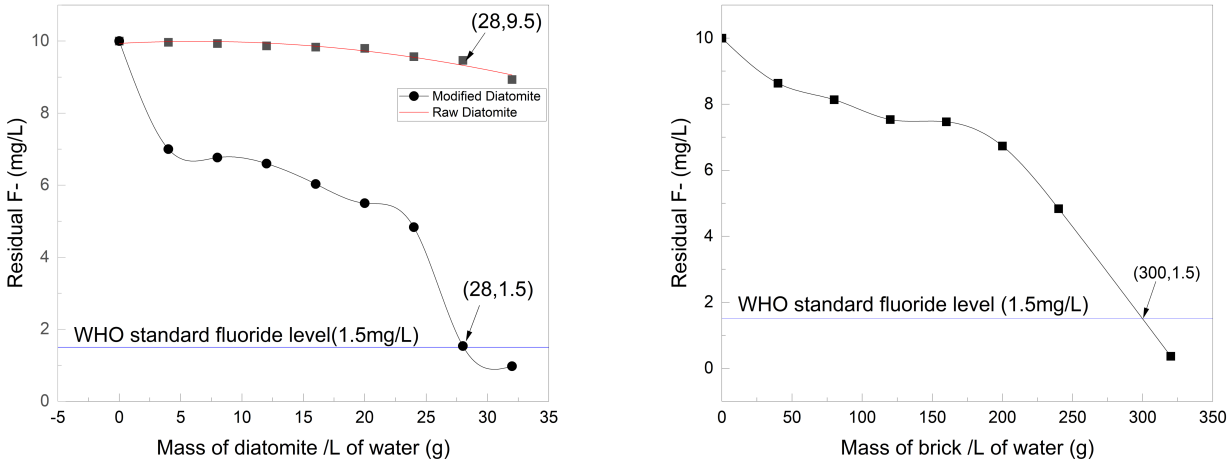

(a) **(b)**

Figure 6. Fluoride removal by diatomite and brick samples (a) Raw and modified diatomite. Modification of the diatomite surface greatly improves its fluoride removal capacity (b) Brick

3.4. Response Surface Methodology

The experimental outcome of the design of experiment together with the predicted outcome is presented in Table 2. The predicted outcome is with respect to the quadratic model presented in Equation 3.1. With the consideration of the p-value and the predicted R^2 values, the quadratic model was suggested and chosen in the present study. This model had the highest adjusted R^2 and predicted R^2 (0.9466 and 0.9502 respectively). Similarly, its p-value was the lowest (<0.0001). As observed in Table 2, the model prediction of the residual fluoride in the water closely matches the experimental results.

Table 2. CCD matrix with experimental and predicted residual fluoride

Run	Residual F-: Experimental (mg/L)	Residual F-: Predicted (mg/L)
1	8.00	8.01
2	8.20	8.20
3	4.80	4.34
4	8.00	7.97
5	4.80	4.34
6	8.40	8.40
7	3.80	4.34
8	3.70	4.34
9	7.90	7.95
10	4.60	4.34
11	7.20	7.18
12	7.30	7.25
13	6.60	6.64

Table 3 shows the analysis of variance (ANOVA) results for response surface quadratic model for residual fluoride. From Table 3, we can see that the model was significant. The model F-value of 43.54 implies the model is significant. There is only a 0.01% chance that an F-value this large could occur due to noise. p-values less than 0.0500 indicate model terms are significant. In this case X_1, $X_1{}^2$, and $X_2{}^2$ are significant model terms. Values greater than 0.1000 indicate the model terms are not significant. Although the ($X_1.X_2$) term was not significant, it cannot be dropped because it was part of the model hierarchy. Furthermore, the lack of fit F-value of 0.0086 implies the lack of fit is not significant relative to the pure error. The lack of fit p-value >0.05 indicates the absence of evidence that the model did not fit. There was a 99.87% chance that a lack of fit F-value of this magnitude could occur due to noise.

Table 3. ANOVA for response surface of the quadratic model for residual fluoride

Analysis of Variance Table Partial Sum of squares Type III						
Source	Sum of Squares	df	Mean Square	F value	p value	
Model	37.31	5	7.46	43.54	< 0.0001	significant
X_1: Diatomite	1.88	1	1.88	10.98	0.0129	
X_2: Brick	0.0656	1	0.0656	0.3826	0.5558	
X_1X_2	0.0625	1	0.0625	0.3647	0.5650	
$X_1{}^2$	15.50	1	15.50	90.41	< 0.0001	
$X_2{}^2$	24.26	1	24.26	141.56	< 0.0001	
Residual	1.20	7	0.1714			
Lack of Fit	0.0077	3	0.0026	0.0086	0.9987	not significant
Pure Error	1.19	4	0.2980			
Cor Total	38.51	12				

Table 4 further highlights the summary of the fit statistics of the model. The predicted R^2 value of 0.9502 is in reasonable agreement with the adjusted R^2 of 0.9466. The difference is less than 0.2. On the other hand, the signal to noise ratio (Adeq precision) value of 14.437 indicates an adequate signal. A signal to noise ratio greater than 4 is desirable [36]. This model can therefore be used successfully to navigate the design space.

Table 4. Summary of the fit statistics

Std. Dev.	0.4140	R^2	0.9688
Mean	6.41	Adjusted R^2	0.9466
C.V. %	6.46	Predicted R^2	0.9502
		Adeq Precision	14.4373

The model generated from this design is shown in Equation 3.1.

$$Y = 11.9 - 3.98x10^{-1}X1 - 4.44x10^{-2}X2 - 9.06x10^{-5}X1X2 + 1.13x10^{-2}X1^2 + 1.30x10^{-4}X2^2 \quad (3.1)$$

This equation was used to plot the response surface and the contour shown in Figure 7. Figure 7 presents the interaction of the surface modified diatomite with brick in removing fluoride in water,

with the response being the residual fluoride. The optimization in this case is a minimization problem, with optimum performance being achieved when the residual fluoride in the water is minimum.

From Figure 7, the optima are shown to be obtained when the diatomite dose is close to 18 g, and the brick dose is about 180 g for a liter of fluoride contaminated water, whose initial fluoride concentration is 10 mg/L. Analysis of the experimental data using design expert software with the goal being the minimization of the residual fluoride gave the optimum conditions with a desirability of 0.872. The optimum adsorbent mixture per milligram of initial fluoride in a liter of water was found to be 1.8 g : 17.8 g surface modified diatomite : brick, respectively. This optimized mixture was experimentally tested for fluoride removal and was able to remove fluoride to a residual value of 1.5 mg/L in 1 hour for an initial concentration of 10 mg/L fluoride in the water. This level meets the desired level of fluoride in drinking water. It is clear from these results that mixing the two adsorbents reduces the amount of the surface modified diatomite required in the defluoridation process by approximately 36% (28g to 18g) and the amount required for brick from by approximately 41% (300g to 178g). This reduction in adsorbent requirement is of great significance given that high amount of aluminium - modified diatomite used in defluoridation could pose a concern for the residual aluminium in water. High residual aluminium in water is noted to cause Alzheimer's disease [3].

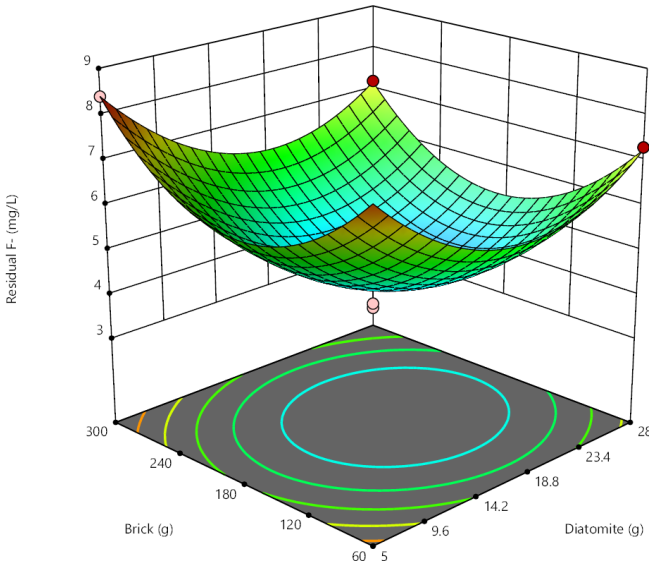

Figure 7. Response surface plot. The effect of brick and surface modified diatomite on removal of fluoride in water (residual fluoride).

3.5. Isotherm studies

The adsorption data was fitted to the adsorption models to understand the adsorption characteristics and the nature of adsorption involved in the individual adsorbents. Both Langmuir and Freundlich isotherms were used in the study because they are useful in describing the adsorption in water and wastewater applications [37, 38]. Figure 8 shows the Langmuir and Freundlich isotherms for the adsorption of fluoride from water by surface modified diatomite and brick. As shown in Figure 8, the adsorption by surface modified diatomite is better explained by the Freundlich isotherm ($R^2 = 0.9753$). This agrees with previous studies, which found the adsorption of fluoride by aluminium hydroxide treated diatomite to involve a multilayer sorption mechanism [22].

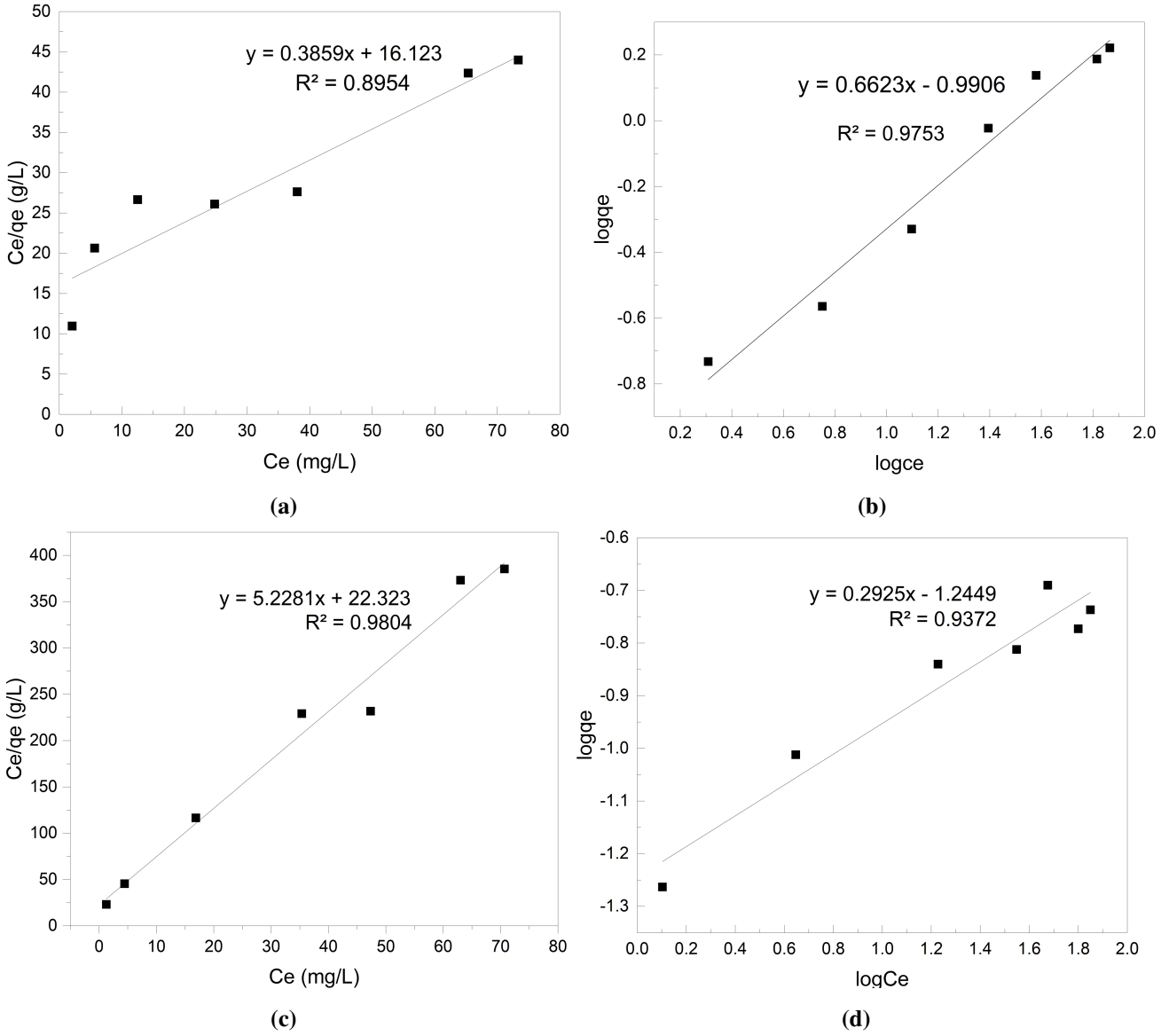

Figure 8. Isotherms for surface modified diatomite and brick, (a,b): Surface modified diatomite, (c,d): Brick, (a,c): Langmuir isotherms, (b,d): Freundlich isotherms. The adsorption was carried out at 20°C and a pH of 6.

The adsorption by brick fit better to the Langmuir isotherm, as shown in in Figure 8c (R^2 = 0.9804), in comparison to the Freundlich isotherm (Figure 8d, R^2 = 0.9372). The assumptions by Langmuir that each site is singly occupied by the adsorbate molecules and that there are no lateral interactions between the adsorbed species are applicable [39]. The present study agreed with a number of previous studies. Priyantha and colleagues in their study of the adsorption behaviour of fluoride on normal brick found the highest regression coefficient on the Langmuir isotherm [40]. Similarly, Kooli and coauthors, while using waste brick to remove basic blue 41 from aqueous solution, found that the removal conformed to the monolayer adsorption isotherm [41].

Table 5 presents the summary of the parameters for both Langmuir and Freundlich isotherms for the surface modified diatomite and brick. From Table 5, the R_L values for both surface modified diatomite and brick indicate favourable sorption of fluoride by both surface modified diatomite and brick ($0 < R_L < 1$) [22]. It is also evident from the qm values that the surface modified diatomite has very high adsorption capacity for fluoride in water (2.59 mg/g), more than 10 times that of brick (0.191 mg/g). This is in agreement with the values of K_F from the Freundlich isotherm, which also suggests high adsorption capacity by the surface modified diatomite due to its large value. The value of 1/n < 1 is indicative of the existence of heterogeneous adsorption surfaces in both diatomite and brick [22]. On the other hand, the high value of 1/n on the surface modified diatomite, as compared to that of brick suggests high bond strength between the adsorbent and the adsorbate for the case of the surface modified diatomite as opposed to brick [42].

Table 5. Calculated Langmuir and Freundlich isotherm parameters

	Langmuir Isotherm				Freundlich Isotherm		
	K_L (Lmg^{-1})	R_L	q_m (mg/g)	R^2	1/n	K_F (mg/g)(mg/L)^n	R^2
Modified Diatomite	0.0239	0.8071	2.5913	0.8954	0.6623	0.1022	0.9753
Brick	0.2342	0.2992	0.1913	0.9804	0.2925	0.0569	0.9372

3.6. Kinetic studies

The experimental data were fitted to both pseudo first-order and pseudo second-order kinetic models in order to understand the adsorption mechanism of fluoride involved on the surface modified diatomite and brick. Figure 9 shows the linear plots of both the pseudo first-order and pseudo second-order models. From Figure 9, it is observed that all the adsorbents followed the pseudo second-order kinetic model in the removal of fluoride. This is evident in the high values of the regression coefficients, for the pseudo second-order model compared to the pseudo first-order model for each of the adsorbents.

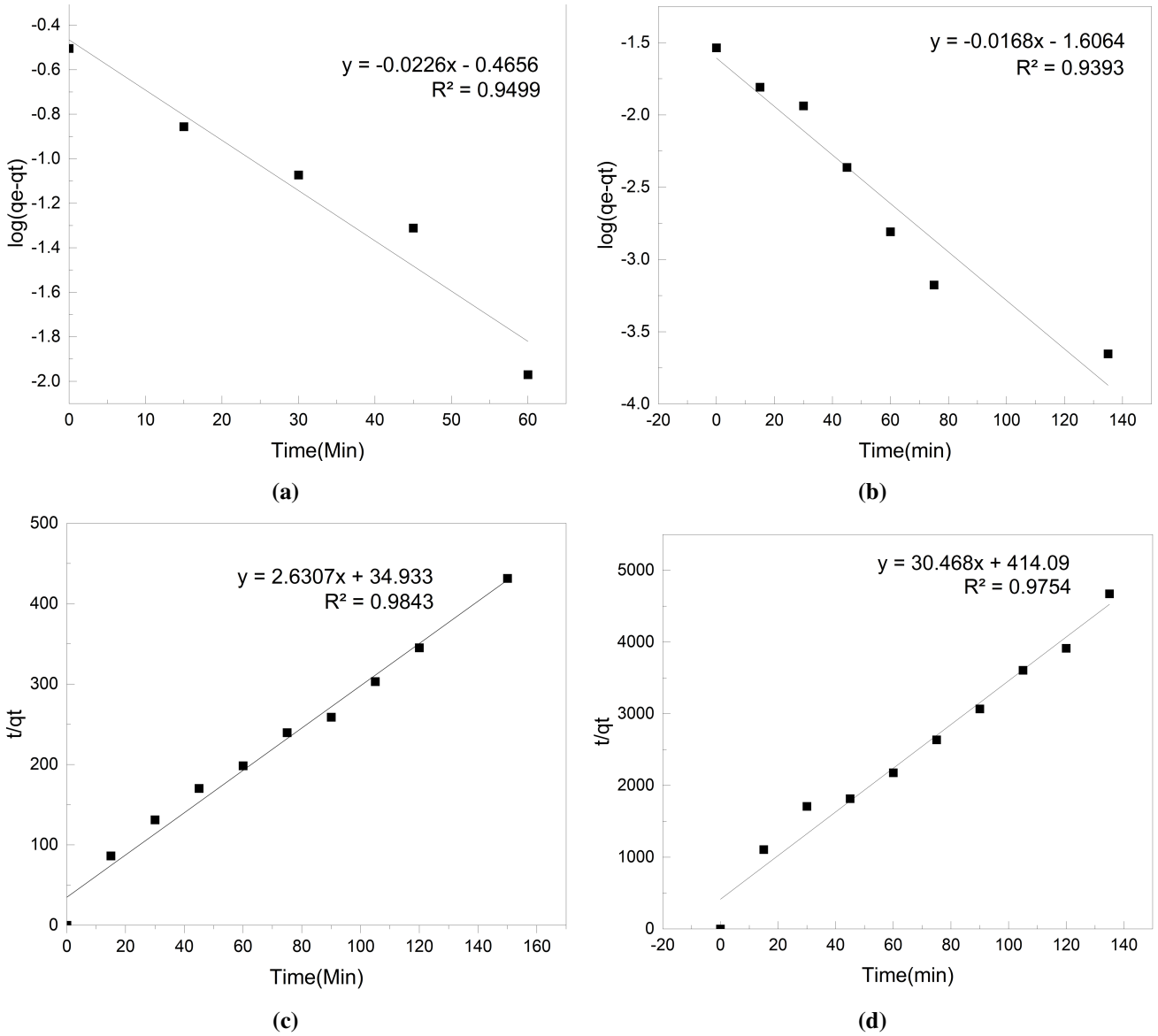

Figure 9. Adsorption kinetics. (a,b) Pseudo first-order kinetic models, (c,d) Pseudo second-order kinetic models, (a,c) Surface modified diatomite, (b,d) Brick. The adsorption was carried out at 20°C and a pH of 6.

Table 6 presents the summary of the kinetic constants from the experiment. From Table 6, the constants indicate the adsorption process by each of the adsorbents favoured the pseudo second-order kinetics model. Other than the high regression coefficients for the pseudo second-order kinetics for each of the adsorbents, the calculated equilibrium capacity of the adsorbents for the pseudo second-order model (q_{e2}) had minor deviation from the experimental equilibrium capacity (q_{eexp}) as compared to the pseudo first-order kinetic model equilibrium capacity (q_{e1}), which largely deviated from the experimental values. The large values of the rate constants K_2 support this. It is therefore clear that the adsorption process by both the brick and the surface modified diatomite involved the chemisorption process, an assumption of the pseudo second-order kinetics [43].

Table 6. Calculated pseudo first-order and pseudo second-order kinetic constants, for the modified diatomite, brick, and optimized mixture.

	Pseudo-first-order			Pseudo-second-order			
	K_1 (min^{-1})	q_{e1} (mg/g)	R_1^2	K_2 ($g.mg^{-1}min^{-1}$)	q_{e2} (mg/g)	R_2^2	$q_e exp$ (mg/g)
Modified Diatomite	0.052	0.3423	0.9499	0.1981	0.3801	0.9843	0.3131
Brick	0.0387	0.0248	0.9393	2.2418	0.0328	0.9754	0.0291
Modified Diatomite + Brick	0.0532	0.0527	0.9315	2.416	0.052	0.9908	0.0490

4. Conclusion

Diatomite samples were modified using aluminium hydroxide and tested for its fluoride removal together with brick. Surface modification of diatomite with aluminium hydroxide greatly improved its fluoride removal capacity. Optimization of a mixture of surface modified diatomite and brick reduced the amount of surface modified diatomite and brick by approximately 36% and 41%, respectively. The reduction in the amount of aluminium hydroxide surface modified diatomite through optimization is of great significance in reducing the potential of high residual aluminium in water. Overall, both surface modified diatomite and brick had favourable sorption for fluoride in water, with chemisorption dominating in both adsorbents. It is therefore clear that an optimized mixture of aluminium-hydroxide surface modified diatomite and brick can be considered for fluoride removal in areas with high fluoride concentration in water.

Further studies on improving the fluoride adsorption by brick should be conducted. Additionally, future research should include the monitoring of the residual aluminium in the treated water when aluminium hydroxide is used for surface modification to ascertain that the treatment process does not leave residual aluminium above the acceptable levels in the water.

Use of AI tools declarationation

The authors declare they have not used Artificial Intelligence (AI) tools in the creation of this article.

Acknowledgements

The authors are grateful to the National Research Fund, Kenya, for supporting this work through its funding on Sustainable Technologies for Potable Water Treatment under Grant Number: 2/MMC/825.

Conflict of interest

The authors report there are no competing interests to declare.

References

1. M Goldberg (2018) Fluoride: double-edged sword implicated in caries prevention and in fluorosis. *J Cell Dev Biol* 1: 10–22.
2. Paul TC Harrison (2005) Fluoride in water: a uk perspective. *J Fluorine Chem* 126:1448–1456.
3. Cyprian Murutu, Maurice S Onyango, Aoyi Ochieng, et al. (2012) Fluoride removal performance of phosphoric acid treated lime: Breakthrough analysis and point-of-use system performance. *Water SA* 38:279–286.
4. Marc J Addison, Michael O Rivett, Helen Robinson, et al. (2020) Fluoride occurrence in the lower east african rift system, southern malawi. *Sci Total Environ* 712: 136260.
5. Paulo Frazão, Marco A Peres, Jaime A Cury (2021) Drinking water quality and fluoride concentration. *Revista de saude publica* 45: 964–973.
6. Habtamu Demelash, Abebe Beyene, Zewdu Abebe, et al. (2019) Fluoride concentration in ground water and prevalence of dental fluorosis in ethiopian rift valley: systematic review and meta-analysis. *BMC Public Health* 19: 1–9.
7. Masoud Ghanbarian, Marjan Ghanbarian, Tayebeh Tabatabaie, et al. (2021) Distributing and assessing fluoride health risk in urban drinking water resources in fars province, iran, using the geographical information system. *Environ Geochem Health* 1–11.
8. Wiem Guissouma, Othman Hakami, Abdul Jabbar Al-Rajab, et al. (2017) Risk assessment of fluoride exposure in drinking water of tunisia. *Chemosphere* 177: 102–108.
9. Piotr Rusiniak, Klaudia Sekuła, Ondra Sracek, et al. (2021) Fluoride ions in groundwater of the turkana county, kenya, east africa. *Acta Geochimica* 40: 945–9601.
10. Steve Mkawale (2021) High levels of fluoride in lake aggravate dental health crisis in baringo. *Standard Media*.
11. Eric Matara (2021) Villagers crippled by lake baringo poisonous waters. *Nation Africa* 1.
12. Joseph K Gikunju, Timothy E Maitho, Jan M Birkeland, et al. (1992) Fluoride in fish from lakes of great rift valley, kenya. *Ecol Food Nutr* 27: 85–90.
13. Enos W Wambu, Gerald Kanyago Muthakia. (2011) High fluoride water in the gilgil area of nakuru county, kenya. 2011.
14. Shikha Modi, Ranjeeta Soni (2013) Merits and demerits of different technologies of defluoridation for drinking water. *J Environ Sci Toxicol Food Technol* 3: 24–7.

15. Karan Dev Jamwal, Deepika Slathia (2022) A review of defluoridation techniques of global and indian prominence. *Curr World Environ* 17: 41–57.

16. Parwathi Pillai, Swapnil Dharaskar, Sivakumar Pandian, et al. (2021) Overview of fluoride removal from water using separation techniques. *Environ Technol Inno* 21: 101246.

17. Shaz Ahmad, Reena Singh, Tanvir Arfin, et al. (2022) Fluoride contamination, consequences and removal techniques in water: a review. *Environ Sci Adv* 1: 620–661.

18. P Senthil Kumar, S Suganya, S Srinivas, et al. (2019). Treatment of fluoride-contaminated water. a review. *Environ Chem Lett* 17: 1707–1726.

19. Carl Francis Z Lacson, Ming-Chun Lu, Yao-Hui Huang (2021) Fluoride-containing water: A global perspective and a pursuit to sustainable water defluoridation management-an overview. *J Clean Prod* 280: 124236.

20. Paripurnanda Loganathan, Saravanamuthu Vigneswaran, Jaya Kandasamy (2013) Enhanced removal of nitrate from water using surface modification of adsorbents–a review. *J Environ Manage* 131: 363–374.

21. Ganesan Sriram, Madhuprasad Kigga, UT Uthappa, et al. (2020) Naturally available diatomite and their surface modification for the removal of hazardous dye and metal ions: a review. *Adv Colloid Interfac Sci* 282: 102198.

22. Tesfaye Akafu, Achalu Chimdi, Kefyalew Gomoro (2019) Removal of fluoride from drinking water by sorption using diatomite modified with aluminum hydroxide. *J Anal Methods Chem* 2019.

23. Majeda AM Khraisheh, Yahya S Al-degs, Wendy AM Mcminn (2001) Remediation of wastewater containing heavy metals using raw and modified diatomite. *Chem Eng J* 99: 177–184.

24. N Selvaraju, S Pushpavanam (2009) Adsorption characteristics on sand and brick beds. *Chem Eng J* 147: 130–138.

25. Arvind Kumar Swarnakar, Shweta Choubey, Santosh K Sar (2007) Defluoridation of water by various technique-a review. *Int J Innov Res Sci Eng Technol* 5: 13174–13178.

26. Sakuni M De Silva, Samitha Deraniyagala, Janitha K Walpita, et al. (2020) Masking ability of various metal complexing ligands at 1.0 mm concentrations on the potentiometric determination of fluoride in aqueous samples. *J Anal Methods Chem* 2020: 1–9.

27. Sumit H Dhawane, Anoar Ali Khan, Kiran Singh, et al. (2018) Insight into optimization, isotherm, kinetics, and thermodynamics of fluoride adsorption onto activated alumina. *Environ Prog Sustain* 37: 766–776.

28. Palanikumar Kayaroganam (2021) *Respon Sur Method Engin Sci*. IntechOpen, Rijeka, Nov 2021.

29. Zhenshun Hong, Yoshitaka Tateishi, Jie Han (2006) Experimental study of macro-and microbehavior of natural diatomite. *J Geotech Geoenviron* 132: 603–610.

30. Anthony A Izuagie, Wilson M Gitari, Jabulani R Gumbo (2016) Defluoridation of groundwater using diatomaceous earth: optimization of adsorption conditions, kinetics and leached metals risk assessment. *Desalin Water Treat* 57: 16745–16757.

31. C Alonso, A Morato, F Medina, et al. (2000) Preparation and characterization of different phases of aluminum trifluoride. *Chem Mater* 12: 1148–1155.

32. Lu Xu, Xueli Gao, Zhaokui Li, et al. (2015) Removal of fluoride by nature diatomite from high-fluorine water: An appropriate pretreatment for nanofiltration process. *Desalination* 369: 97–104.
33. Chiharu Tokoro, Shinya Suzuki, Daisuke Haraguchi, et al. (2014) Silicate removal in aluminum hydroxide co-precipitation process. *Materials* 7: 1084–1096.
34. Xiaowei Ouyang, Liquan Wang, Jiyang Fu, et al. (2021) Surface properties of clay brick powder and its influence on hydration and strength development of cement paste. *Constr Build Mater* 300: 123958.
35. Asheesh Kumar Yadav, CP Kaushik, Anil Kumar Haritash, et al. (2006) Defluoridation of groundwater using brick powder as an adsorbent. *J Hazard Mater* 128: 289–293.
36. Anil Kumar, Abraham Chirchir, Saul S Namango, et al. (2022) Microwave irradiated transesterification of croton megalocarpus oil–process optimization using response surface methodology. In *Proceed Sustain Res Innov Confer* 132–137.
37. K Kadirvelu, C Karthika, N Vennilamani, et al. (2005) Activated carbon from industrial solid waste as an adsorbent for the removal of rhodamine-b from aqueous solution: Kinetic and equilibrium studies. *Chemosphere* 60: 1009–1017.
38. V Gomez, MS Larrechi, MP Callao (2007) Kinetic and adsorption study of acid dye removal using activated carbon. *Chemosphere* 69: 1151–1158.
39. Abhas Jain, SK Singh (2014) Defluoridation of water using alum impregnated brick powder and its comparison with brick powder. *Int J Eng Sci Innov Technol* 3: 591–6.
40. N Priyantha, C Senevirathna, P Gunathilake, et al. (2009) Adsorption behavior of fluoride at normal brick (nb)—water interface. *Int J Environ Protec Sci* 3: 140–146.
41. Fethi Kooli, Yan Liu, Mostafa Abboudi, et al. (2019) Waste bricks applied as removal agent of basic blue 41 from aqueous solutions: base treatment and their regeneration efficiency. *Appl Sci* 9: 1237.
42. Andy Proctor, J.F. Toro-Vazquez (2019) Chapter 10 - the freundlich isotherm in studying adsorption in oil processing. In Gary R. List, editor, *Bleaching and Purifying Fats and Oils (Second Edition)* 209–219. AOCS Press, UK, second edition edition, 2009.
43. Mahir Alkan, Özkan Demirbaş, Mehmet Doğan (2007) Adsorption kinetics and thermodynamics of an anionic dye onto sepiolite. *Micropor Mesopor Mat* 101: 388–396.

AIMS Press